

A SEGMENTED NEUTRON DETECTOR BASED ON SILICON-PIN PHOTODIODES USING NEUTRON-PROTON CONVERTERS

by

Ahmet BAYRAK, Mete YUCEL, Esra BARLAS YUCEL, and Cenap S. OZBEN*

Department of Physics Engineering, Faculty of Science and Letters, Istanbul Technical University, Istanbul, Turkey

Scientific paper

<https://doi.org/10.2298/NTRP181229014B>

A segmented neutron detection system based on windowless silicon-PIN photodiodes has been designed and tested with various hydrogen rich converter materials. Each channel from the segmented structure uses an independent custom-made low noise charge sensitive preamplifier and an OPAMP based shaping amplifier. Signals from each channel were digitized using a fast, single bit digitizer and the pulses from each channel were simultaneously recorded with an FPGA board. An AmBe neutron source was used for the test measurements and relative neutron detection efficiencies were determined. This low-cost detector can be used for monitoring fast neutrons in reactors, accelerator facilities or medical centers using neutron therapy.

Key words: neutron detection, polyethylene, proton, silicon-PIN photodiode

INTRODUCTION

Radiation detection has improved significantly since the discovery of Geiger Mueller detectors. They provide easy and fast access for monitoring the gamma and beta rays. There have been continuing efforts for improving and stabilizing their operational conditions [1, 2]. Special considerations must be taken into account to extend the lifetime of the detectors and any method to predict the life span of the radiation detectors is appreciated [3]. However, new solid state devices such as silicon-PIN (Si-PIN) photodiodes have been widely used for detecting ionizing radiation especially for the last decade and they encounter a wide range of applications, from the measurements of environmental radiation [4, 5] to X-ray imaging [6, 7] and other types of nuclear radiation [8-11]. These detectors can also be used at accelerator facilities for beam loss monitoring and safety purposes in beam tunnels [12].

Since all detectors have a lifetime, the techniques used for determining lifetime is an important issue and Si-PIN photodiodes can be used for the detection of neutrons when a special converter material is used [13-16]. Some of the examples are the studies about detecting explosive materials [16-19]. In one of these studies, Geant-4 simulations were performed with segmented Si-PIN detectors for the detection of underground explosives and the results showed that

this device was capable of detecting neutrons when a neutron to charged particle converter was used. Our work is a complementary study in terms of building up and testing the neutron detector proposed by Yucel *et al.* [19].

The ^{10}B and ^6LiF are widely used materials for converting thermal neutrons to charged particles [20-22]. They emit alpha particles and tritons, respectively, followed by the absorption of thermal neutrons by nuclei. In case of fast neutrons, polyethylene $(\text{C}_2\text{H}_4)_n$ is one of the most frequently used converter materials because of its high hydrogen content and availability [13, 21, 23, 24].

Fast neutrons knock out the protons from hydrogen and they can reach a silicon detector positioned next to the converter material and deposit energy in it. Studies showed that the production and absorption rate of the secondary particles becomes more or less constant above a certain thickness (usually a few hundreds of microns) [25]. For that reason, the converter materials to be tested were chosen to be thicker than 1 mm.

Most detector designs using Si-PIN photodiodes are limited to use a single sensor with a relatively small active surface area. The electronics and control units of these designs are mostly made from commercially available and expensive equipment. Some custom-made designs are available as in references [23], [26]. We aimed to develop a detector with a relatively large area for neutron detection by implementing nine photodiodes, each having a 1 cm² active area and independent digital readouts.

* Corresponding author; e-mail: ozben@itu.edu.tr

DETECTOR HARDWARE

The detector circuit is based on two main components. The first part is the signal electronics where the deposited energy of the incoming particle is converted into an electrical signal. The second stage is the hardware for transferring the count information to a memory unit by a microprocessor. This microprocessor in this case is an field programmable gate array (FPGA) and the data is stored in the memory of a Raspberry Pi module for further processes. This section is named as the *Control and Readout Electronics*. Figure 1 shows the designed detector.

SIGNAL ELECTRONICS

The very first element of the signal electronics is the PS100- CER-PIN2 produced by First Sensor [27]. This photodiode is windowless, having a 5 nA dark current and 80 pF terminal capacitance under a 12 V reverse bias. Its noise equivalent power is $3 \cdot 10^{-14} \text{ W/ Hz}$. When fast neutrons hit the converter material, an incident proton is ejected due to inelastic collision of the neutron with hydrogen. Since the proton is charged, it deposits energy in the silicon structure by ionizing its surrounding, generating electrons and holes through their path. The electric field provided from the reverse bias potential drives the electrons and the holes into the cathode and anode, respectively. However, the elec-

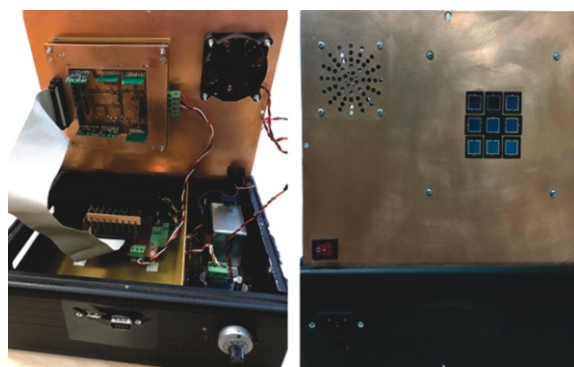


Figure 1. Pictures of the detector array and its electronics

trons generated in the intrinsic region results in a net current. This small current is amplified properly with a charge sensitive preamplifier. Figure 2 shows the block diagram of the signal electronics. Figure 3 shows the schematics and the printed circuit board of the charge sensitive preamplifier used in the signal electronics section. The circuit was originally developed by the Instrumentation Division of the Brookhaven National Laboratory [28]. However, the printed circuit board was redesigned with the equivalent JFET due to non-availability of the original ones. The shaping amplifier has a standard R-C design and the fine tuning was performed experimentally. Figure 4 shows the schematics and the printed circuit board of the shaping amplifier.

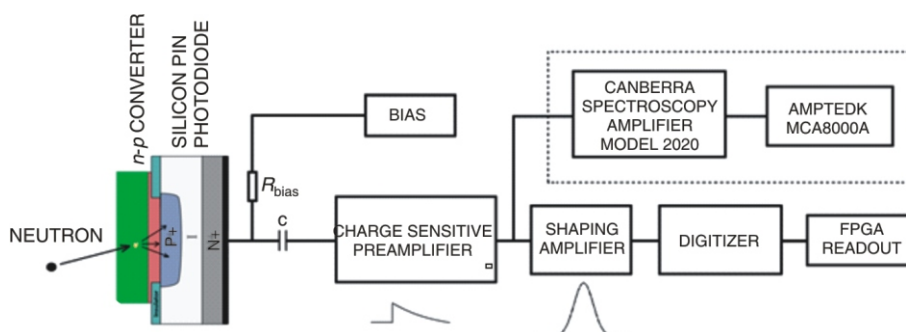
CONTROL AND READOUT ELECTRONICS

The main part of the control and readout electronics is a Xilinx Spartan 3AN FPGA module. Together with the sub-modules designed in the FPGA, it performs the counting process for a predetermined period of time and then transmits the data to a computer. The counting process can be started, stopped or reset by the user commands transmitted through a Python graphical user interface.

Counting operations are performed with nine independent counter modules set inside the FPGA running with a clock signal of 100 MHz providing 10 ns time resolution. In addition, an edge detector implementation was performed for each channel to detect the pulses. Afterwards, the counting process is performed and 24-bit data is stored in the memory locations for each channel separately. When the measurement period is completed, 24 bit data for each channel is divided into three parts each having 8 bits.

Following the data transmission from the FPGA, a Raspberry Pi single board computer receives individual bytes through a Python script. All incoming bytes are read, organized and stored in individual files for each channel. This kind of data storage is useful when continuous periodical measurements take place and the data analysis becomes easier for independent channels.

Figure 2. Block diagram of the signal electronics



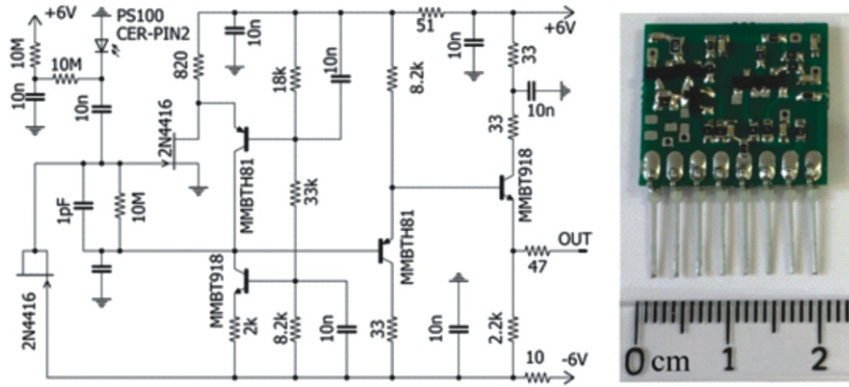


Figure 3. The schematics and printed circuit board of the charge sensitive preamplifier

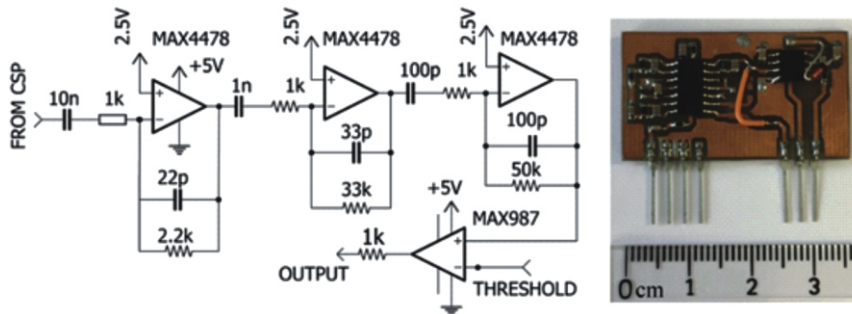


Figure 4. The schematics and printed circuit board of the shaping amplifier

In reality, the detector does not require the use of an FPGA to monitor the neutron count rate. However, FPGA has very flexible programming tools which can be very useful for signal shape analysis. For instance, alpha, beta, gamma, neutron, proton signals can be separated from each other by their pulse shapes.

MEASUREMENTS

Several measurements took place for determining the performance of the detector. Alpha, gamma, and neutron sources were used for measuring the response of the detector to various types of radiation. The Canberra 2020 spectroscopic amplifier and Amptek MCA 8000A were used in addition to our instrumentation for spectroscopic measurements.

Measurements with ²²⁶Ra

The first measurement took place for obtaining the energy spectrum of ²²⁶Ra. It has 4.6 MeV and 4.784 MeV alpha lines with 5.5 % and 94.5 % relative intensities, respectively [29]. Figure 5 shows the alpha spectrum of ²²⁶Ra. Because of the poor energy resolution, the mentioned alpha lines are indistinguishable. The cluster of counts at lower energy is due to the scattering and energy loss of alpha particles in the cylindrical metal enclosure of the source. The ²²⁶Ra emits a 186 keV characteristic gamma line. The merge plot in

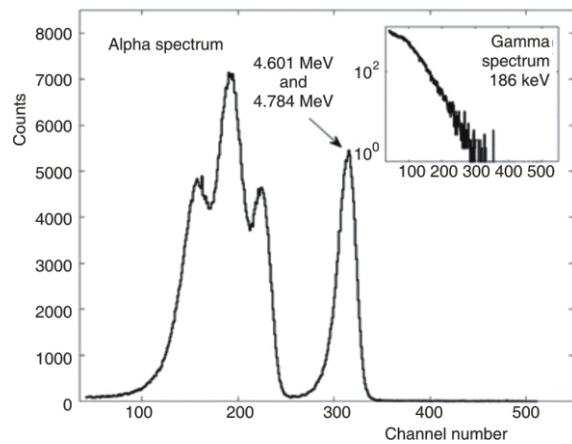


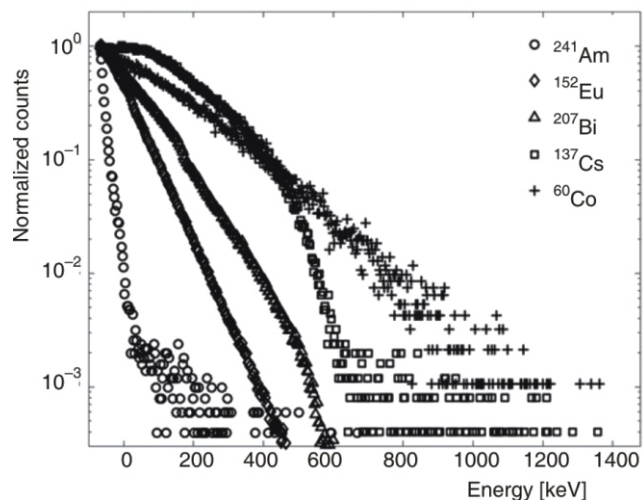
Figure 5. Spectrum of ²²⁶Ra

fig. 5 shows the gamma spectrum of the source. This spectrum was taken with a 0.1 mm thick polyethylene absorber to remove the alpha particles and the amplifier gain was set 10 times higher.

Measurements with gamma sources

Although this detector was not designed for gamma measurements, it can detect gamma rays with relatively low efficiency. However, despite of its low efficiency, this device can also be used for monitoring gamma rays with high intensity.

Figure 6. Spectra of gamma sources of ^{60}Co , ^{137}Cs , ^{152}Eu , ^{237}Bi and ^{241}Am gamma sources



Gamma measurements with ^{60}Co , ^{137}Cs , ^{152}Eu , ^{237}Bi , and ^{241}Am standard sources were performed. Gamma spectra from these sources are shown in fig. 6. Each spectrum was taken using a single segment and sources were positioned directly on the top of the PIN detector. However, since the activity of ^{137}Cs was relatively higher compared to the other sources, it is positioned 5 cm above the detector element to reduce the pileup events. All spectra were normalized to unity height as shown. Energy calibration was performed from the determination of endpoints of ^{241}Am , ^{137}Cs , and ^{60}Co spectra. These sources have strong gamma lines at 59.6 keV, 661.6 keV, and 1252.9 keV (as the average of 1173.2 keV and 1332.5 keV of ^{60}Co), respectively. The ^{60}Co was also used in the energy calibration since the detection efficiency is similar at both 1173.2 keV and 1332.5 keV and these gamma lines are equally intense. The linear calibration curve is given in fig. 7 to prove ^{60}Co was acceptable for the energy calibration. The ^{237}Bi has gamma lines at 569.7 keV, 1063.7 keV, and 1770 keV and their intensities are 98 %, 75 %, and 7 %, respectively [26]. Since detection efficiency is relatively larger at low energies, it is expected that the endpoint of the spectrum of ^{237}Bi is

dominated by the 569.7 keV gamma line. This is exactly what one can see from fig. 6. A similar argument holds for ^{152}Eu but it is more complicated to explain since it has many strong gamma lines ranging from 121.8 keV to 1408.0 keV.

Measurements with neutron sources

Neutron measurements took place using the J. L. Sheppard Am-Be neutron source with 3 Ci ^{241}Am activity. The ^{241}Am has a strong gamma line at 59.5 (%35.9) keV which is highly detectable by a 300 m Si-PIN detector. Figure 8 shows the spectra taken at the irradiation port of the Howitzer type Am-Be source. The 59.5 keV gamma contribution to the Am-Be spectrum can be seen from the low energy part of the spectrum. Gamma rays are emitted from the excitation of ^{12}C produced from the bombardment of beryllium with alpha particles as the following interaction.

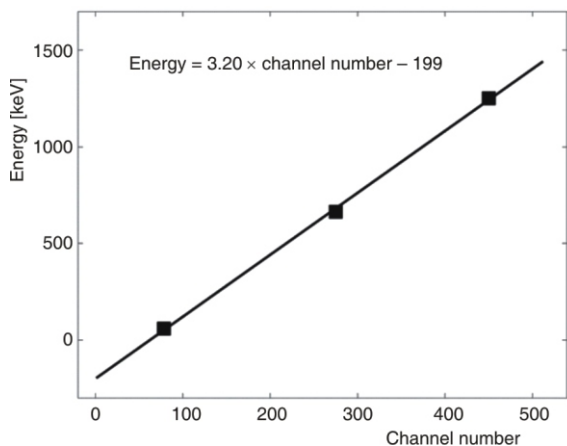
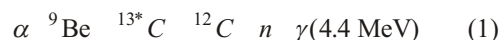


Figure 7. Energy calibration using ^{60}Co , ^{137}Cs , and ^{241}Am gamma sources

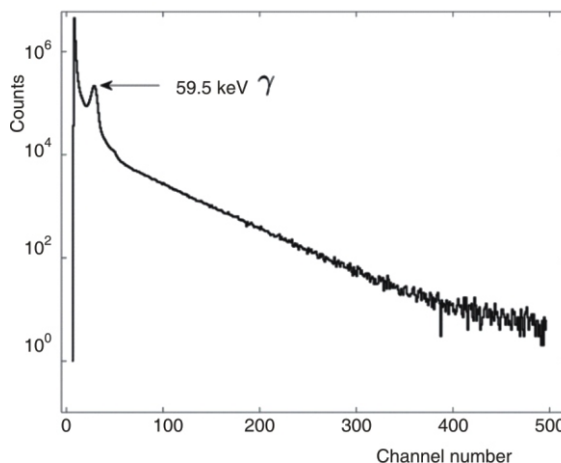


Figure 8. Spectra of the Am-Be neutron source

Table 1. Counts compared from the two measurements. The measurement time was set to 30 minutes

	No converter	FR4	Plexiglas	Silicon	HDPE	Paraffin
FPGA	1500	2954	2992	3074	3038	3147
MCA	1412	2863	3034	3096	2960	3157

Measurements with neutron to proton converters:

High density polyethylene (HDPE), fiberglass cloth with epoxy resin (FR4), silicon, plexiglas, and paraffin were used as converter materials. These materials were attached in front of the detector array and exposed to neutrons by positioning it perpendicular to the axis of the irradiation port of the Am-Be neutron source. Detector source distance was around 50 cm at the irradiation position.

The data taking for the measurements took place with two independent methods. The first one was based on the charge sensitive preamplifier given in fig. 3 and the Canberra 2020 spectroscopic amplifier. The amplifier is then connected to an Amptek MCA-8000A for spectral measurements. Connection of FPGA was also established for 9 detectors independently and the data from each detector were collected and stored during the measurements. Shaping amplifiers given in fig. 4 were used when the data were collected with FPGA. The shaping times were different for both data collection methods and therefore the noise background was slightly higher for the FPGA based detection system. Integral MCA counts above channel 58, corresponding to 280 mV in the 5V scale, provided comparable results with hard thresholded FPGA. Table 1 shows the comparison of MCA and FPGA counts with and without the converter materials. The measurements were performed for 30 min. Figure 9 shows the comparison of the naked neutron spectrum and the spectra obtained when various converter materials were used. As seen from the figure, there are visible differences in the detected spectra especially at high energies. Spectra above channel 200 is due

to the contribution of protons produced from fast neutrons in the converter materials.

To determine the most sensitive region from the spectral measurements for the separation of fast neutrons, each spectrum in fig. 9 was integrated between a variable lower level discriminator (LLD) and channel 1024. New data sets for each case in fig. 9 were reconstructed with incremental steps between 21 and 300. Data sets for the converter materials were then normalized to the one obtained without a converter. Figure 10 shows the results from this procedure.

Figure 10 shows that the optimum fast neutron separation channel is 200 for all converter materials. Above 200, the statistics become limited.

UNCERTAINTIES

Since the purpose of this study was to concentrate on the instrumentation rather than the precise measurements, the statistical and systematical uncertainties were not studied in detail. However, we would like to mention the sources of possible uncertainties of our measurement procedure qualitatively. Uncertain-

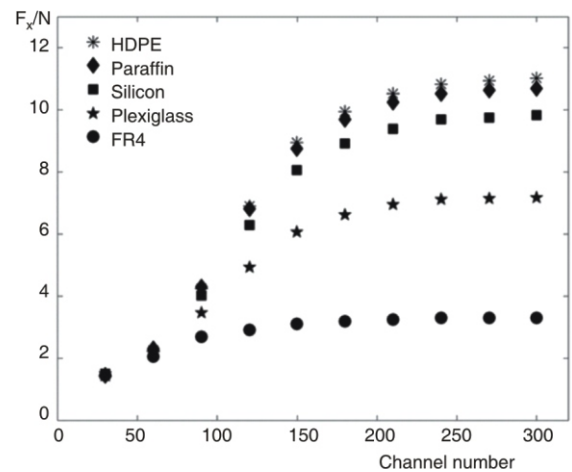


Figure 10. Ratio of the integral counts above LLD with and without the converters

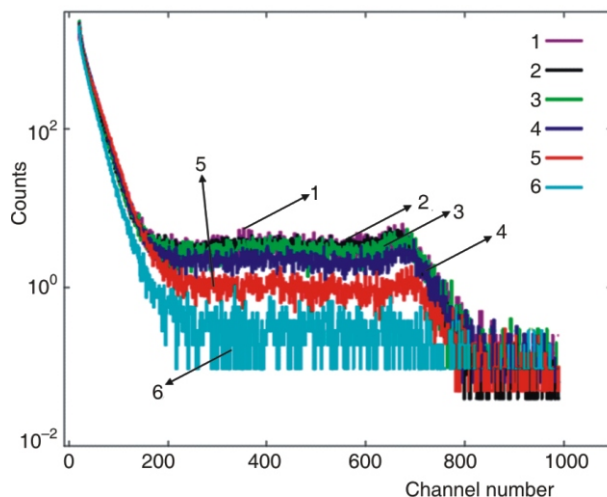


Figure 9. Spectra of the Am-Be source with various converter materials; 1 – Paraffin, 2 – HDP, 3 – Silicon, 4 – Plexiglas, 5 – FR4, 6 – No converter used

ties in the measurements can be classified as statistical and systematic errors. The work [30] describes the sources of uncertainties very well. One of the sources of our systematic error is due to the calibration of the detector. Pileup had the most disturbing effect on the energy calibration procedure. The activity differences between the standard sources resulted in a different pileup contribution to the spectra from each source. However, changing the detector-source distance, especially for relatively active ^{137}Cs , helped to reduce the pileup dramatically. Endpoint calibration was performed by fitting the flat region of each spectrum to reduce the uncertainty of the energy calibration. The uncertainty due to cosmic rays is very small since the thickness of the photodiode is only 300 μm and there is small probability for an energetic muon to deposit its energy even partially. In any neutron based measurement, the background due to 59.5 keV gamma rays from the Am-Be neutron source was considerably below the spectral region where the calculations for neutrons took place.

CONCLUSIONS

This work showed that the detector and the instrumentation presented in this study can be used for measuring the gamma rays and fast neutrons. The system can also be used for detecting alpha and beta radiations.

Fast neutron detection is only possible when a hydrogen rich converter material is used. Conversion efficiency was observed to be similar for all converters.

A large active area and the novel signal readout electronics are the achievements which are not available for most of the studies in previously mentioned literature. This device can be useful in scattered neutron measurement applications [19]. Especially the flexible signal readout offers the possibility of extending the active area to a much bigger size by additional channels. Additionally, a large detection area can be advantageous where neutron monitoring is crucial (*i. e.*, reactors, accelerators, and medical centers).

AUTHORS' CONTRIBUTIONS

The instrumentation setup, the coding, the measurements and the analysis were carried out by A. Bayrak as the main part of his Ph.D thesis. M. Yucel and E. B. Yucel validated our measurements with their simulations. The manuscript was written by A. Bayrak and C. S. Ozben.

REFERENCES

[1] Perazic, L. S., et al., Application of an Electronegative Gas as a Third Component of the Working Gas in the

Geiger-Mueller Counter, *Nucl Technol Radiat*, 33 (2018), 3, pp. 268-274

[2] Obrenović, M. D., et al., Statistical Review of the Insulation Capacity of the Geiger-Mueller Counter, *Nucl Technol Radiat*, 33 (2018), 4, pp. 369-374

[3] Arbutina, D. S., et al., Aging of the Geiger-Mueller Counter Due to Particle Conductance in an Insulating Gas, *Nucl Technol Radiat*, 32 (2017), 3, pp. 250-255

[4] Bayrak, A., et al., A Complete Low Cost Radon Detection System, *Applied Radiation and Isotopes*, 78 (2013), Aug., pp. 1-9

[5] Voytchev, M., et al., The Use of Silicon Photodiodes for Radon and Progeny Measurements, *Health Physics*, 80 (2001), 65, pp. 90-96

[6] Emirhan, E., et al., A Low Cost X-Ray Imaging Device Based on BPW-34 Si-PIN Photodiode, *Nuclear Instruments and Methods in Physics Research Sec. A: Accelerators, Spectrometers, Detectors and Associated Eq.*, 819 (2016), May, pp. 1-5

[7] Kanno, I., et al., Two-Dimensional TransXend Detector with Band Structure Absorbers for Third-Generation Energy-Resolved Computed Tomography with Improved Spatial Resolution, *Journal of Nuclear Science and Technology*, 54 (2017), 1, 22-29.

[8] Kim, K. H., et al., Development of Alpha Detector Module based on Large Area PIN Photodiode, *Journal of Nuclear Science and Technology*, 45 (2008), 5, pp. 417-420

[9] Cho, Y. H., et al., Comparative Study of a CsI and a ZnSe (Te/O) Scintillation Detectors Properties for a Gamma-ray Measurement, *Journal of Nuclear Science and Technology*, 45 (2008), 5, pp. 534-537

[10] Andjelković, M. S., et al., Feasibility Study of a Current Mode Gamma Radiation Dosimeter Based on a Commercial PIN Photodiode and a Custom Made Auto-Ranging Electrometer, *Nucl Technol Radiat*, 28 (2013), 1, pp. 73-83

[11] Huang, P., et al., Energy Response Correction for an Electronic Personal Dosimeter Using the Channel Ratio Method, *Nuclear Science and Techniques*, 28 (2017), 7, p. 101

[12] Hou, L., et al., Beam Loss Monitor System for SSRF Storage Ring, *Journal of Nuclear Science and Technology*, 45 (2008), 5, pp. 425-427

[13] Hosono, Y., et al., Fast Neutron Detector Using PIN-Type Silicon Photodiode, *Nuclear Instruments and Methods in Physics Research Section A: Accelerators, Spectrometers, Detectors and Associated Equipment*, 361 (1995), 3, pp. 554-557

[14] ***, Measurements of Fluxes of Thermal Neutrons Using Detector $^6\text{LiI}(\text{Eu})\text{-Si-Pin-Pd}$ and a Charge-Sensitive Preamplifier, IEEE Nuclear Science Symposium. (Nalcioglu, O.)

[15] ***, Recent Results from Thin-Film-Coated Semiconductor Neutron Detectors, International Symposium on Optical Science and Technology, (James, R. B., Franks, L. A., Burger, A., Westbrook, E. M., Durst, D. D., Westbrook, E. M., Durst, R. D.)

[16] Totsuka, D., et al., Performance Test of Si PIN Photodiode Line Scanner for Thermal Neutron Detection, *Nuclear Instruments and Methods in Physics Research Section A: Accelerators, Spectrometers, Detectors and Associated Equipment*, 659 (2011), 1, pp. 399-402

[17] ***, Heavy Scintillators for Scientific and Industrial Applications, *Proceedings*, CRISTAL 2000 International Workshop, Edition Frontiers, Chamonix, France, 1992, pp. 144-146

[18] Fioretto, E., et al., CsI (Tl)-photodiode detectors for γ -Ray Spectroscopy, *Nuclear Instruments and Methods in Physics Research Sec. A: Accelerators, Spectrometers, Detectors and Associated Equipment*, 361 (1995), 3, pp. 554-557

- trometers, Detectors and Associated Eq., 442 (2000), 1-3, pp. 412-416
- [19] Yucel, M., et al., Simulations of Si-PIN Photodiode Based Detectors for Underground Explosives Enhanced by Ammonium Nitrate, *Nuclear Instruments and Methods in Physics Research Sec. A: Accelerators, Spectrometers, Detectors and Associated Eq.*, 88 (2018), Feb., pp. 152-157
- [20] Voytchev, M., et al., Neutron Detection with a Silicon PIN Photodiode and 6LiF Converter, *Nuclear Instruments and Methods in Physics Research Sec. A: Accelerators, Spectrometers, Detectors and Associated Eq.*, 512 (2003), 3, pp. 546-552
- [21] Adamiec, G., et al., Response of a Silicon PIN Photodiode to an Am-Be Neutron Source, *Nuclear Instruments and Methods in Physics Research Sec. A: Accelerators, Spectrometers, Detectors and Associated Eq.*, 534 (2004), 3, pp. 544-550
- [22] Kang, K. H., et al., Response of a Photodiode Coupled with Boron for Neutron Detection, *Journal of the Korean Physical Society*, 65 (2014), 9, pp. 1374-1378
- [23] ***, Evaluation of a PIN Photodiode Detector in Neutron Gamma Fields, AIP Conference Proceedings. (Patterson, M.)
- [24] ***, Characterization of a Neutron Spectrometer Based on a PIN Photodiode, Workshop on Radiation Dosimetry: Basic Technologies, Medical Applications, Environmental Applications, (Zanini, A.)
- [25] Mesquita, C. H., Hamada, M. M., Development of Neutron Detector Using the PIN Photodiode with Polyethylene (n, p) Converter, *IEEE Transactions on Nuclear Science*, 50 (2003), 4, pp. 1170-1174
- [26] Yang, H., et al., Evaluation of a Lil (Eu) Neutron Detector with Coincident Double Photodiode Readout, *Nuclear Instruments and Methods in Physics Research Sec. A: Accelerators, Spectrometers, Detectors and Associated Eq.*, 652 (2011), 1, pp. 364-369
- [27] ***, Datasheet of PS100-7-CER-2 PIN photodiode, First Sensor Corporation, <https://www.first-sensor.com/en/products/optical-sensors/detectors/pin-photodiodes/>, 2012
- [28] ***, Fiddling Carbon Strings with Polarized Proton Beams, AIP Conference Proceedings, (Meyer, T. S., Webber, R)
- [29] ***, The Lund/LBNL Nuclear Data Search [Internet], Berkeley, USA: LBNL, <http://nucleardata.nuclear.lu.se/toi/>
- [30] Stanković, K. D., et al., Influence of Tube Volume on Measurement Uncertainty of GM Counters, *Nucl Technol Radiat*, 25 (2010), 1, pp. 46-50

Received on December 29, 2018

Accepted on April 23, 2019

Ахмет БАЈРАК, Мете ЖУЏЕЛ, Есра БАРЛАС ЖУЏЕЛ, Џенап С. ОЗБЕН

СЕГМЕНТИРАНИ НЕУТРОНСКИ ДЕТЕКТОР ЗАСНОВАН НА СИЛИКОН-PIN ФОТОДИОДАМА КОЈИ КОРИСТИ НЕУТРОН-ПРОТОНСКЕ ПРЕТВАРАЧЕ

Сегментирани неутронски детекциони систем заснован на силикон-PIN фотодиодама без прозора пројектован је и испробан са различитим конверторским материјалима обogaњеним водоником. Сваки канал сегментираних структуре користи израђен по мери претпојачавач ниског шума осетљив на наелектрисања и појачавач ОРАМР типа. Сигнали из сваког канала дигитализовани су коришћењем брзог, једнобитног дигитајзера, те су импулси из сваког канала симултано записани помоћу FPGA плоче. За тест мерења коришћен је AmBe неутронски извор и одређена је релативна ефикасност детекције неутрона. Овај детектор ниске цене може се користити за мониторинг брзих неутрона у реакторима, акцелераторским постројењима, или медицинским центрима са неутронском терапијом.

Кључне речи: детекција неутрона, полиетилен, протон, Силикон-PIN фотодиода